ORIGINAL ARTICLE

Impacts of scenarios RCP4.5 and RCP8.5 on plant physiology in Tapajos National Forest in the Brazilian Amazon using the ED2.2 model

Luciana Cristina de Sousa VIEIRA[1]*[iD], Antonio Ocimar MANZI[2], Vicente de Paula SILVA[1], Prakki SATYAMURTY[3], Vanessa de Almeida DANTAS[1], Aldeize da Silva SANTOS[3]

[1] Instituto Nacional de Pesquisas Espaciais, Estr. do Fio 5624-6140, Mangabeira, Eusébio, 61760000, Ceará, Brazil

[2] Instituto Nacional de Pesquisas Espaciais, Avenida dos Astronautas, 1.758 - Jd. Granja - CEP 12227-010, São José dos Campos – SP, Brazil

[3] Instituto Nacional de Pesquisas da Amazônia, Av. André Araújo 2936, Petrópolis, Manaus, 69080971, Amazonas, Brazil

* Corresponding author: vieirameteorologia@gmail.com; [iD] https://orcid.org/0000-0003-3115-825X

ABSTRACT

Models that simulate the process of stomatal conductance (gs) for a given set of environmental conditions are important, as this process is the main mechanism that controls the gas exchange of terrestrial plants absorbing atmospheric CO_2 in tropical forests. Simulations were performed for the Tapajós National Forest, in the western Brazilian Amazon, observing the gs process under the current climate scenario (control) and under the scenarios RCP4.5 and RCP8.5 (2071 – 2100), using the ED2.2 ecosystem demography model. The results showed that the lower availability of soil water for the plants reduced photosynthesis due to the closing of the stomata. The model results for gross primary productivity (GPP) are similar to those observed in the field, varying about ≈24 MgC ha^{-1} year^{-1} for the rainy season and ≈23 MgC ha^{-1} year^{-1} for the dry season (average 2002 to 2010) in the control scenario. In the RCP4.5 scenario, simulated GPP was 30.7 and 30 MgC ha^{-1}year^{-1} for the rainy and dry season, respectively (30.5 and 25 MgC ha^{-1}year^{-1}, respectively, for the RCP8.5 scenario). Our results also show that there may be a limitation on the increase in biomass carbon with the concentration of CO_2, as GPP was lower in RCP8.5, despite this scenario having a higher value of atmospheric CO_2 relative to RCP4.5.

KEYWORDS: biomass, climate change, IPCC, leaf

Impactos dos cenários RCP4.5 e RCP8.5 na fisiologia vegetal na Floresta Nacional do Tapajós, na Amazônia brasileira, através do modelo ED2.2

RESUMO

Modelos que simulam o processo de condutância estomática (gs) para um determinado conjunto de condições ambientais são importantes, pois esse processo é o principal mecanismo que controla as trocas gasosas das plantas terrestres ao absorver o CO_2 atmosférico em florestas tropicais. Realizamos simulações para a Floresta Nacional do Tapajós, na Amazônia Ocidental brasileira, observando o processo da gs sob o cenário climático atual (controle) e sob os cenários RCP4.5 e RCP8.5 (2071 – 2100) usando o modelo demográfico de ecossistema ED2.2. Os resultados mostraram que a menor disponibilidade de água no solo para as plantas reduziu a fotossíntese devido ao fechamento dos estômatos. Os resultados do modelo para produtividade primária bruta (PPB) foram semelhantes aos observados em campo, variando cerca de ≈24 MgC ha^{-1} ano^{-1} para a estação chuvosa e ≈23 MgC ha^{-1} ano^{-1} para a estação seca (média 2002 a 2010) no cenário controle. No cenário RCP4.5, o resultado da PPB simulado foi de 30,7 e 30 MgC ha^{-1}ano^{-1} para as estações chuvosa e seca, respectivamente (30,5 e 25 MgC ha^{-1} ano^{-1}, respectivamente, para o cenário RCP8.5). Nossos resultados mostram que pode haver uma limitação no aumento do carbono da biomassa com a concentração de CO_2, uma vez que a PPB foi menor no RCP8.5, apesar deste cenário ter um valor maior de CO_2 atmosférico em relação ao RCP4.5.

PALAVRAS-CHAVE: biomassa, mudanças climáticas, IPCC, folha

INTRODUCTION

Over the past two decades, an increase of 0.2 °C per decade in the Earth´s surface temperature has been observed, leading to global climate change (Hawkins *et al.* 2017). Although the climate varies naturally over time and space, the observed temperature increase has been much faster than the pace recorded over glacial and interglacial cycles, and the best explanation for this increase is the accumulation of greenhouse gases in the atmosphere, mainly due to the increase in the concentration of atmospheric CO_2 (Nobre *et al.* 2007).

Climate change scenarios such as RCP4.5 and RCP8.5 (RCP, Representation Concentration Levels) have been used in numerous simulations, as they project a future with a higher concentration of atmospheric CO_2 (Lyra *et al.* 2016). The climate projections used in this study were obtained from the forced ETA model with the outputs of the English global model HadGEM3 by Chou *et al.* (2014). The ETA model was developed at the University of Belgrade and is used by INPE for forecasting weather (Bustamante *et al.* 1999) and climate (Chou *et al.* 2005). The Eta-HadGEM2-ES Regional Climate Model provides a set of climate projections (RCP's) for South America for the period 1960-2005 (present climate) and 2070-2099 (future projections).

The consequences of the increase in CO_2 have been investigated in several studies. An increase in CO_2 levels can affect plant physiology, causing stomata to open less with high concentrations of CO_2 (Field *et al.* 1995), which directly reduces the flow of moisture to the atmosphere (Sellers *et al.* 1996). In rainforest regions like the Amazon, where a significant portion of the moisture for precipitation comes from surface evaporation, the reduction of stomatal opening can also contribute to a decrease in precipitation, resulting in reduced soil moisture and surface and subsurface runoff, leading to a reduction in river flow and the so-called hydrological drought, in addition to meteorological drought (Betts *et al.* 2004; Liberato *et al.* 2010). There are four possible effects of drought in a tropical forest: (a) xylem embolism, which affects the carbohydrate transport capacity of trees (McDowell *et al.* 2011; Anderegg *et al.* 2012); (b) hydraulic fatigue (Rowland *et al.* 2015); (c) continuous reduction of carbohydrate reserves (Doughty *et al.* 2015); and (d) an increase of the fragility of the system with each drought, known as the degradation hypothesis (Franklin *et al.* 1985).

Another effect that the accumulation of CO_2 in the atmosphere causes is the retention of infrared radiation emitted from the Earth's surface after the absorption of sunlight, leading to a continuous increase in global surface temperatures (Zandalinas *et al.* 2021). This heating can reduce vegetation growth, altering the thermal environment of plants (Piao *et al.* 2009; Ficklin and Novick 2017). The temperature increase predicted by the Intergovernmental Panel on Climate

Change (IPCC) scenarios can increase the evapotranspiration, leading to a reduction in soil moisture (Liberato *et al.* 2010).

Vegetation dynamics models that simulate the effects of climate change on tropical forests are becoming increasingly robust, by including the interactions of biophysical, physiological and structural parameters with meteorological variables (Saleska *et al.* 2009; Islam *et al.* 2021). One such simulation framework is the terrestrial biosphere model ED2.2 (Ecosystem Demography), which considers the heterogeneity of the ecosystem, increasing the capacity of the model to simulate the differential growth of plants as a function of size, age, density, leaf area etc. (Moorcroft *et al.* 2001).

Our objective was to evaluate the effect of scenarios RCP4.5 and RCP8.5 on stomatal conductance and gross primary productivity in the ED2.2 model for a tropical forest area in the Amazon.

MATERIAL AND METHODS

Study area

The modeling simulation was carried out for an area (acronym FNT/K67) of the conservation unit Tapajós National Forest (Flona Tapajós), an area of 590,000 ha located at km 67 of the BR-366 highway, in the state of Pará (54º58'W, 2º51'S), Brazil. Most rainfall occurs between January and June (rainy season), with little or no rain in the dry season (De Souza *et al.* 2017).
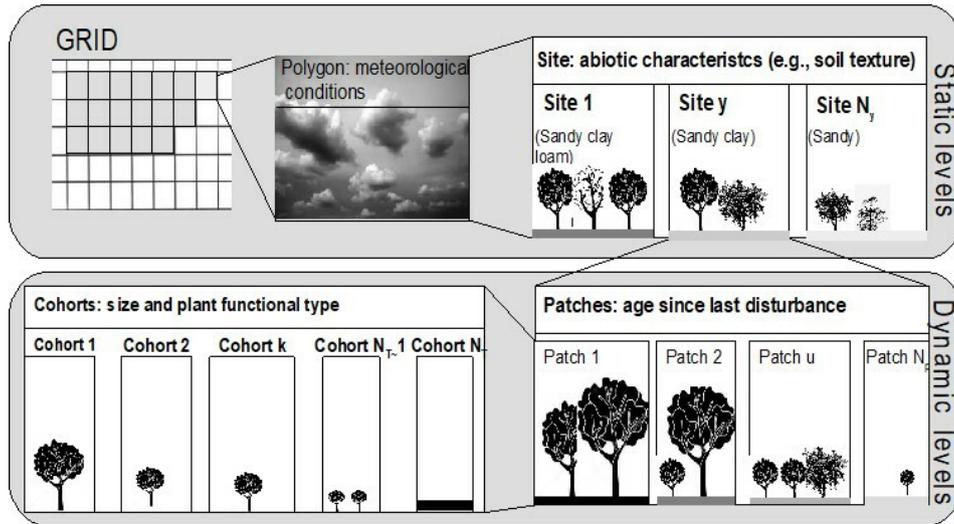
The model

The Ecosystem Demography model (ED2.2) simulates the dynamics of continental ecosystem structure and functioning on a local scale, representing the population of trees. The model was built with a hierarchical structure that represents the physical and biological heterogeneity of the ecosystem, dividing the domain of interest into polygons (Longo *et al.* 2016). In each polygon, the meteorological forcing above the canopy is spatially uniform. The number of polygons is determined at the beginning of the simulation and is fixed in time. Each polygon is subdivided into "Sites". Each "Site" is subdivided into "Patches". Within each "Patch", there are structures called "Cohorts", which are groups of trees with different sizes and population densities (Figure 1).

Input data

For the initial configuration of the model, we used three types of input data: (I) atmospheric conditions (meteorological data), (II) edaphic conditions (data on soil properties); and (III) initial state of the vegetation (forest inventory data), which are described below.

Meteorological data – Specific air temperature (K) and humidity (kg kg^{-1}), molar fraction of CO_2 (µmol mol^{-1}), air pressure (Pa) above the crown, precipitation rate (kg m^2 s^{-1}), solar radiation flux and long wave radiation incident on the

Figure 1. Simplified illustration of the multiple hierarchical levels in the ED2.2 ecosystem demography model, organized by static levels (grid, polygons and sites) and dynamic levels (patches and cohorts). Adapted from Longo *et al.* (2019).

surface (W m^{-2}), and horizontal wind speed (m s^{-1}) were obtained for 2002-2009 from a micrometeorological station (hourly data) located within Flona Tapajos.

Soil properties – Soil data for Flona Tapajós was obtained from Nepstad *et al.* (2002), the soil being of sandy-clayey type, with 0.59 clay and 0.39 sand. Soil porosity, residual moisture and field capacity data were obtained from Bruno *et al.* (2006), from a 8-m soil profile obtained from observations at depths of 8.000, 6.959, 5.995, 5.108, 4.296, 2.890, 1.780, 0.960, and 0.020 m.

Soil relative humidity (%) was calculated for each layer using equation 1.

$$\vartheta_k = \frac{v_{k} - v_{\Re}}{v_{PO} - v_{\Re}} \tag{1}$$

where υ is the soil moisture for layer k, $v_{\Re}$ is the residual soil moisture (m³w.m^{-3}) and v_{PC} is the porosity.

The soil hydraulic parameters, porosity, matrix potential for porosity, wilting point, logarithmic slope of the water retention curve and hydraulic conductivity, were derived from pedotransfer functions based on soil granulometry (Cosby *et al.* 1984). The flow of water between soil layers occurs in the liquid phase and was determined by Darcy's law (Bonan 1996). The field capacity in the model was calculated based on the equation of Clapp and Hornberger (1978). Permanent wilting point and residual soil moisture were defined as the soil moisture at which the soil matrix potential is equivalent to -1.5 and -3.1 Mpa, respectively (Longo *et al.* 2016).

The values of matrix potential at saturation and soil moisture at saturation fluctuate both seasonally and with soil depth according to the volume of rainfall that recharges the system. Despite defining a moisture value at the beginning

of the simulations, the value of these parameters will vary with soil moisture.

Plant productivity – Forest inventory data from Flona Tapajós were obtained from Espírito-Santo *et al.* (2005). They are leaf area index, tree height and density observed at six transects per hectare. Gross primary productivity (GPP) is the vegetation's ability to capture atmospheric CO_2 while losing some of this assimilated CO_2 through autotrophic respiration (Silva 2013). In the ED2.2 model, GPP (kg C plant^{-1} s^{-1}) was calculated using equation 2.

$$GPP_m = \frac{M_c \#_m \Lambda_m}{n_m} \cdot \left[\left(1 - 0_{g,\pi_m}\right)\dot{A}_{0,m} + 0_{g,\pi_m}\dot{A}_{l^*,m} + \dot{D}_m \right] \tag{2}$$

where M_c = the molar mass of carbon; n_m = the population density (plant m^{-2}); $\#_m$ = 1 for plants with stomata on one side of the leaf; Λ_m = the leaf area index (m² m^{-2}); $0_{g,\pi_m}$ = weighting between closed and open stomata; $\dot{A}_{0,m}$ = photosynthesis if the stomata are closed; $\dot{D}_m$ = photosynthesis if the stomata are open, breathing in the dark.

Plant respiration (kg C plant^{-1} s^{-1}) is calculated with equation 3:

$$R_{\lambda m} = \frac{M_c \#_m \Lambda_m}{n_m} \cdot D_m \tag{3}$$

Plant physiology – The stomatal conductance (gs) for C3 plants was calculated according to Leuning (1995) using equation 4. The gs controls water loss and the CO_2 assimilation rate (m s^{-1}).

$$g_s = \begin{cases} \dfrac{MA_o}{(C_s - t)\left(1 + \dfrac{D_s}{D_o}\right)} + b & for\ open\ stomata \\ b & for\ closed\ stomata \end{cases} \tag{4}$$

where M and D_o are empirical constants and b is the cuticular conductance. Ds represents the water vapor deficit

$D_s = e_L - e_S$ and e_L is the intercellular water vapor concentration, assumed to be at saturation (Medvigy *et al.* 2009).

The water limitation in the model was calculated according to equations 5 and 6 (Medvigy *et al.,* 2009).

$$A_{net} = f_{o,w}A_o + (1 - O_{g,\pi_m})A_c \qquad [5]$$

$$\psi_{net} = f_{o,w}\psi_o + (1 - O_{g,\pi_m})\psi_c \qquad [6]$$

where A_{net} = instantaneous rate of photosynthesis (mol$_c$ m^{-2} leaf^{-1}); ψ_{net} = plant evapotranspiration (mol$_w$ m^{-2} leaf^{-1}). $f_{o,w}$ is the weighting for open stomata, A_o and A_c stand for photosynthesis for open stomata and for closed stomata, respectively.

A_{net} and ψ_{net} are considered to be linearly related under conditions of open stomata (A_o, ψ_o) and closed stomata (A_c, ψ_c), weighted by the plant's water availability (supply) relative to its total water demand. The weight that determines when the stomata are open (O_{g,π_m}) is given by equation 7.

$$O_{g,\pi_m} = \frac{1}{1 + \frac{demand}{supply}} \qquad [7]$$

where $demand = \psi_o SLA\ Bleaf$; SLA = specific leaf area; Bleaf = leaf biomass; $supply = K_W W_{avail,tot}\ broot$; where the is $W_{avail,to'}$ = total amount of water accessible to the vegetation layer; broot = the vegetation layer's total C in fine roots; and K_W = constant.

The radiation in the model is solved using a multi-layer version of the two-stream model applied to three broad spectral bands: photosynthetically active radiation (PAR, wavelengths between 0.4 and 0.7 µm), near-infrared radiation (NIR, wavelengths between 0.7 and 3.0 µm) and thermal infrared radiation (TIR, wavelengths between 3.0 and 15 µm (Longo *et al.* 2016). The evaporation rates between the leaf and soil surface with canopy air space are regulated by two factors, the aerodynamic resistance and the effective vapor pressure deficit (VPD) between the respective surfaces and the air space. The variables related to water flow in the model are precipitation, runoff, throughfall, transpiration, leaf interception, wood interception and drainage. The allometric equation that defines root depth relative to tree height in ED2.2 is given by the simplified exponential function:

$$z\rho = -1.114DBH^{0.422}, \qquad [8]$$

where DBH = tree diameter at breast height (cm).

Simulations

To assess the equilibrium state of the vegetation biomass, simulations were performed to adjust the initial conditions to the model's equations, in a process called spin-up (Yang *et al.* 1995). The model ran for a spin-up period of 300 years. To assess the equilibrium state of the forest, we assumed that the last 30 years of simulation corresponded to quasi-equilibrium conditions. The non-instability of the model was assessed through the analysis of the seasonality of soil moisture, GPP and gs in relation to the field observations (Restrepo-Coupe *et al.* 2013; Nepstad *et al.* 2013; Da Rocha *et al.* 2004). After the simulations for the control scenario, scenarios RCP4.5 and RCP8.5 were simulated in the model.

To simulate the rainfall and air temperature conditions for Flona Tapajós projected by the RCP scenarios, a descriptive statistical analysis was performed comparing two time intervals from the Eta-HadGEM2-ES model: 1960-2005 (historical data) and 2070-2099 (model projections). The comparison showed an increase in air temperature and a reduction in rainfall (Table 1). After defining the values in Table 1, they were used to change the model's input data. For example, the RCP4.5 scenario estimate an increase in air temperature of 4°C, so we add 4°C to the monthly values. For rain and specific humidity, the data were also modified according to increase (+) or decrease (-). In RCP4.5 we kept the CO_2 concentration at 650 ppm and in RCP8.5 at 1100 ppm, with a constant value of longwave radiation for each scenario. The specific humidity (q) was calculated using temperature and relative humidity and its variation between the periods was assessed through descriptive statistics.

Table 1. Longwave radiation and atmospheric CO_2 concentration settings for two climate-change scenarios and projection of variation in meteorological parameters in 2070-2099 relative to 1960-2005 in Tapajós National Forest (Brazilian Amazon). Air temperature (T_air = air temperature; LWR = longwave radiation; PRP = rainfall; q = specific humidity; and CO_2 concentration. +increase, and - indicates decrease relative to 1960-2005.

Scenario	T_air (ºC)	PRP (%)	q (%)	CO$_2$ (ppm)	LWR (W m^{-2})
RCP4.5	+4	-17	+13	650	22.40
RCP8.5	+7.5	-30	+7	1100	41.40

The run time chosen for the simulations with the RCP4.5 and RCP8.5 scenarios was nine years, based on the simulated equilibrium data, generating new data for the interval from 2002 to 2010. The initial condition of soil moisture distribution was used as the simulations control for vegetation dynamics. Validation was performed with soil moisture data obtained in the field by Nepstad *et al.* (2013) for January 2002 to December 2004. Part of the water that reaches the ground through the leaves (throughfall) dripping and run-off from the wood (wood interception) runs off the surface and the rest seeps into the soil (drainage).

The radiation budget is solved using a multi-layer version of the two-stream model applied to three broad spectral bands: photosynthetically active radiation (PAR, wavelengths between 0.4 and 0.7 µm), near-infrared radiation (NIR,

wavelengths between 0.7 and 3.0 μm) and thermal infrared radiation (TIR, wavelengths between 3.0 and 15 μm (Longo *et al.* 2019).

RESULTS

Soil moisture

The vertical profiles of moisture represented well the annual variability of soil moisture observed in the field (R^2 = 0.89) (Figure 2). The seasonal pattern of soil moisture responded to precipitation. The ED2.2 model values for soil moisture were similar to the observed data, but the differences were larger in deeper layers (from layer 5 downwards). The reason could be that the soil was classified as a mineral in the ED2.2 model, although the soil in the study area contains organic matter and macropores (Furtado Neto *et al.* 2013).
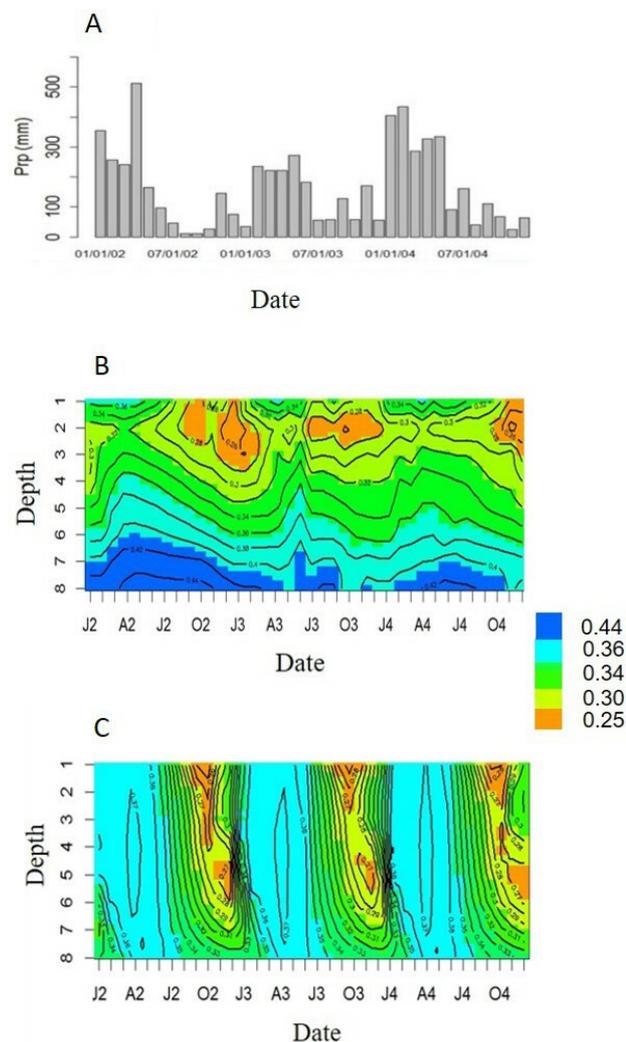
Figure 2. Monthly rainfall (A) and mean monthly volumetric soil moisture (m³ m⁻³) interpolated for an 8-m soil profile in Tapajós National Forest for the interval from January 2002 to December 2004, according to field data (B) and model data (C). This figure is in color in the electronic version.

In this version of the model organic matter in the soil is not taken into account.

In the control scenario, the moisture was recharged throughout the profile to the deeper layers as soon as the rainy season began (Figure 3a). In the RCP4.5 scenario, there was a reduction in soil moisture, especially in the deeper layers, most markedly around 8 m, with values around 0.25 m³ m⁻³ (Figure 3b).

The moisture reduction in the layers around 5 m indicates the depth at which absorption of water by plant roots is greatest at these levels. The reduction of soil moisture occurred due to the reduction in rainfall, the only entry of water into the system. In the RCP8.5 scenario, the deeper layers remained with humidity below 0.25 m³ m⁻³, providing humidity for plant roots up to 4 m deep (Figure 3c). The distribution of the roots in the model reached up to 5 m deep, which may explain the greater dryness around this depth. In the ED2.2, the allometric equations assume that smaller trees have shallower roots than larger trees. As a result, during years of normal rainfall, the soil moisture is recharged down to the deeper soil layers during the wet season and is an important source of water for taller trees during the dry season. As the model allows the presence of roots in several layers, they have a uniform distribution along the profile, which is not supported by field data, due to the limited information on root structure at the species level for the Amazon.

The vapor pressure deficit was positively correlated with the higher soil matrix potential (R^2 = 0.85), suggesting that water stress reduced the ecosystem's efficiency in using available water.

For the control scenario, the transpiration simulated by the model was 75.7 mm month⁻¹ in the rainy season and 83.9 mm month⁻¹ in the dry season (Table 2). In the RCP4.5 scenario, transpiration was 52.5 mm month⁻¹ in the rainy season and 73.9 mm month⁻¹ in the dry season, while the respective values in the RCP8.5 scenario were 51.1 and 62.5 mm month⁻¹. The amount of water lost by transpiration in the model, is considered to be exactly equal to the amount of soil water brought into the intercellular space of the leaf through the plant's vascular system.

The decrease in rainfall in the two RCP scenarios had a direct effect on the generation of runoff (Table 2). In the three scenarios, transpiration increased from mid-March and May, when the amount of water available to the plant in the soil reached the maximum peak of the season. As transpiration increases and peaks around September, the water available to the plant gradually decreases and peaks at a minimum around September as well. The lowest transpiration value in the rainy season was recorded approximately two months after the water available to the plant reached its minimum (end of the dry season). In scenarios RCP4.5 and RCP8.5, there was

A

B

C
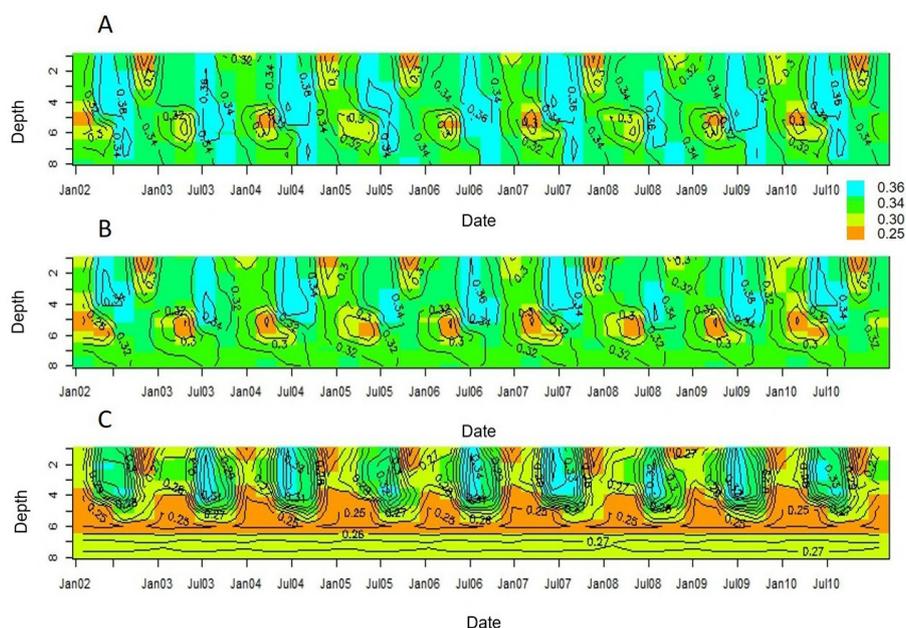
Figure 3. Average monthly volumetric values of soil water (m³ m⁻³) interpolated for eight layers of an 8-m soil profile in Tapajós National Forest for the control scenario (A), and the RCP4.5 (B) and RCP8.5 (C) climate-change scenarios. Data for the period January 2002 to December 2010. This figure is in color in the electronic version.

Table 2. Average of water balance components (mm month⁻¹) for the control scenario and the RCP4.5 and RCP8.5 simulated climate-change scenarios in Tapajós National Forest in the dry and rainy over a period of nine years (2002 – 2010).

Variable	Control		RCP4.5		RCP8.5	
	Dry	Rainy	Dry	Rainy	Dry	Rainy
Precipitation	66.5 ± 0.9	251.0 ± 0.2	55.5 ± 0.8	210.4 ± 0.7	46.8 ± 0.4	177.5 ± 0.6
Throughfall	3.8 ± 0.2	15.5 ± 1.1	1.9 ± 0.9	8.2 ± 0.4	1.9 ± 0.9	8.3 ± 0.6
Transpiration	83.9 ± 0.6	75.7 ± 0.3	73.9 ± 0.4	52.5 ± 0.6	62.5 ± 0.8	51.1 ± 0.4
Leaf interception	58.5 ± 0.17	219 ± 0.1	49.0 ± 0.1	184.9 ± 0.16	41.4 ± 0.2	155.8 ± 0.18
Wood interception	4.2 ± 0.06	15.7 ± 0.11	4.6 ± 0.09	17.3 ± 0.1	3.4 ± 0.5	13.3 ± 0.6
Runoff	2.5 ± 0.08	18.9 ± 0.07	1.8 ± 0.1	8.9 ± 0.1	0.7 ± 0.1	3.5 ± 0.09
Drainage	38.3 ± 0.14	34.4 ± 0.1	17.3 ± 0.12	8.1 ± 0.09	0.17 ± 0.12	0.07 ± 0.1

a reduction in transpiration (Table 2) as the severity of the drought increased.

GPP and sensitive and latent heat flow

The simulation resulted in a GPP of 25 ± 0.76 Mg C ha⁻¹ year⁻¹, close to the value of 25.6 Mg C ha⁻¹ year⁻¹ obtained for Tapajós by Restrepo-Coupe *et al.* (2013). In the three simulations, GPP hourly averages were higher between 11:00 and 13:00 (Figure 4a) when PAR reached maximum values. The correlation coefficient between GPP and PAR was $R^2 = 0.9$ for all scenarios. GPP reached higher values in the RCP8.5, followed by RCP4.5 and the control scenario (Figure 4a).

GPP varied most markedly between seasons in the RCP8.5 scenario. Monthly average soil water storage explained about 50-60% of the variation in GPP (R^2 = 0.46, 0.5 and 0.6 for the control, RCP4.5 and RCP8.5 scenarios, respectively). These results are similar to published studies using the ED2.2

model (Longo *et al.* 2016). Powell *et al.* (2013) showed that the GPP data simulated by the ED model for the Tapajós area was underestimated. This can be explained, perhaps, by the fact that seasonality in the model does not yet capture the drop in productivity during the transition from the dry to the rainy season. However, despite these details that are still under study, the model reasonably represents what would be expected in terms of GPP for the study site.

The simulated GPP for the RCP4.5 and RCP8.5 scenarios was 30.7 and 30.5 Mg C ha⁻¹ year⁻¹ for the rainy season, and 30 and 25 Mg C ha⁻¹ year⁻¹ for the dry season, respectively. Our simulated values for gs during the day significantly decreased from 16:00 (Figure 4b). VPD was higher in the RCP4.5 and RCP8.5 than in the control scenario (Figure 4d). The equation for gs used in the model is regulated by the vapor pressure deficit, which explains the opposite behavior between gs and VPD. GPP was strongly correlated with gs ($R^2 \sim 0.9$ in all the

three scenarios). When the leaf temperatures were higher, gs tended to be lower (Figure 4b,c). The lowest gs values were observed for the RCP8.5, followed by the RCP4.5 scenario. VPD was highest between 12:00 and 15:00 (Figure 4d). In the control scenario, the maximum values of VPD were around 2.5 kPa and they are higher in the rainy season (Figure 4d).

The latent heat flux decreased and the simulated sensible heat flux increased, both in the dry and rainy season (Table 3), responding to the increase in CO_2 concentration and increase in air temperature.

DISCUSSION

Our results from the ED2.2 model showed that the reduction in precipitation under the conditions of the RCP4.5 and RCP8.5 scenarios can directly impact soil moisture. Severity was accentuated in the RCP8.5 scenario, despite higher atmospheric CO_2 concentration and increase in water use efficiency, indicating that a drier and warmer climate can limit vegetation growth. The variability in water availability can affect tree growth rates, since precipitation is the main source of soil moisture and, consequently, of water for vegetation and the values of soil hydraulic parameters depend on soil granularity (Longo *et al.* 2019). In the model, for any soil moisture, the hydraulic conductivity tended to be higher for sandy than for clayey soils. However, as clay particles are smaller, the soil matric potential reaches the wilting point much faster in clayey soils. In addition, the hydraulic conductivity is much lower for sandy soils than for clayey soils at the same matric potential (Longo *et al.* 2019).

The reduction of rainfall can potentially lead to a lower entry of water into the soil, increasing the matric potential. This matric potential indicates the effort that the plant will make to extract water from the soil, and stomatal conduction is directly related to this variable through a factor on a phenomenological scale (O_{g,π_m}) ranging from 0 (no stress) to 1 (maximum stress) (Longo *et al.* 2016).

Decreased soil water reduced stomatal conductance and transpiration in scenarios RCP4.5 and RCP8.5. This behavior is a result of increased water stress, increased vapor pressure deficit and increased air temperature (Longo *et al.* 2016). In nature, stomatal closure blocks the flow of CO_2 to the leaves, affecting the accumulation of photoassimilates, which can reduce productivity (Paiva *et al.* 2005). Simulations

Table 3. Monthly energy balance components in the dry and rainy season for a control and two climate-change scenarios (RCP4.5 and RCP8.5) simulated for a nine-year period (2002 - 2010) in the Tapajós National Forest. Average value for the dry and rainy season. LE = latent heat flux; H = sensible heat flux (W m^{-2}). Values are the mean ± standard deviation.

Variable	Dry season	Rainy season
	Control	
LE	100.34± 3	93 ± 5
H	76 ± 6	53 ± 6
	RCP4.5	
LE	100 ± 3.4	88 ± 4.7
H	77.42 ± 5.2	56 ± 5.5
	RCP8.5	
LE	94.82 ± 7.9	80 ± 9.5
H	78.94 ± 7.7	58 ± 8.2
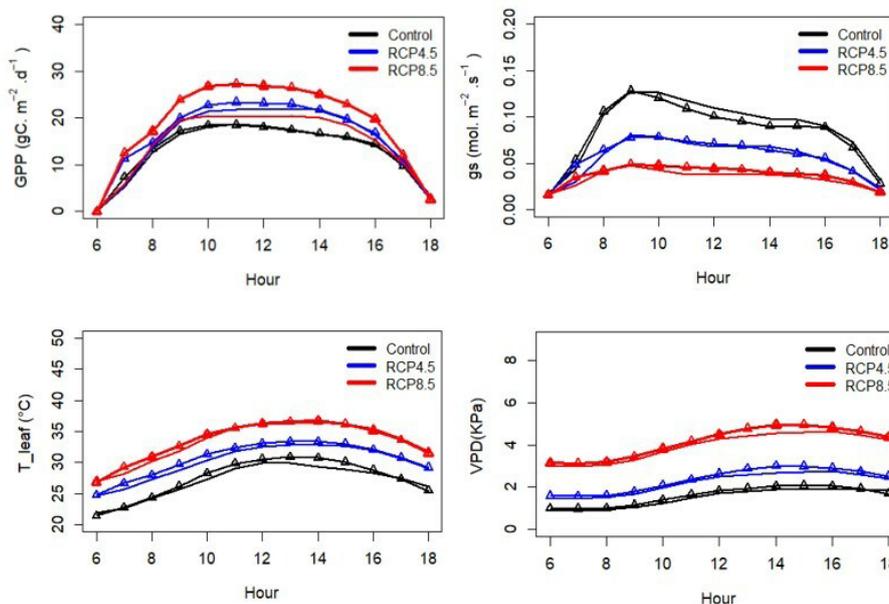
Figure 4. Average hourly diurnal variation (6 am - 18 pm) of vegetation productivity and physiological parameters in Tapajos National Forest over the period of January 2002 to December 2010 for a control scenario and two climate-change scenarios. A – gross primary productivity (GPP); B – stomatal conductance (gs); C – leaf temperature (t_leaf); D – vapor pressure deficit (VPD). Plain lines represent the dry period and lines with triangles the rainy season. This figure is in color in the electronic version.

of the CMIP5 (Coupled Model Intercomparison Project) indicated that the increase in atmospheric CO_2 can reduce local evapotranspiration in tropical forest regions, decreasing stomatal conductance and transpiration, reducing the flow of moisture to the atmosphere, which may affect 69% of the precipitation in the Amazon (Kooperman *et al.* 2018). Therefore, in addition to the decreased reduction in forest growth that is directly linked to the reduction in CO_2 absorption, the lower stomatal conductance in the Amazon reduces local evapotranspiration, directly impacting precipitation. In the field data from the study site, gs decreased between 15:00 and 16:00, and gs decreases with increasing leaf temperature (Felsemburgh 2009).

The increase in VPD with ambient temperature can affect photosynthesis, leading to the closing of stomata, reducing transpiration and, with it, decreasing CO_2 assimilation and photosynthetic rate (Lloyd and Farquar 2008). This result was obtained by Felsemburgh (2009) in Tapajós. In tropical forests, in the dry season, VPD is less than ~0.2 kPa and can increase to ~0.7 kPa in the rainy season (Rocha *et al.* 2014). When the VPD increased with temperature, the GPP decreased due to the decrease in soil water. This sensitivity to temperature rise is not the same for all species, due to differences in photorespiration rates. In C3 plants, CO_2 assimilation depends on carbon gain via the bifunctional enzyme Rubisco (oxygenase/carboxylase) and CO_2 loss via photorespiration and mitochondrial respiration (Braga *et al.* 2021). Thus, increased photorespiration and mitochondrial respiration may limit carbon assimilation rates in C3 plants at high temperatures (Braga *et al.* 2021).

Autotrophic and heterotrophic respiration have important roles in the impact of drought on the forest. Covariance tower estimates suggest that, in the dry season, there is a reduction in respiration in the forest in the Tapajós area (Restrepo-Coupe *et al.* 2017). The seasonality of the ED model for ecosystem respiration is almost exclusively driven by the seasonality of heterotrophic respiration, with a significant decline in the dry season, due to lower soil moisture (Powell *et al.* 2013).

Regarding GPP, the model algorithm would need a CO_2 absorption function based on field data to represent more accurately the forest dynamics in a scenario of increased atmospheric CO_2. The values were close to the value of 25.6 Mg C ha^{-1} year^{-1} obtained for Tapajós by Restrepo-Coupe *et al.* (2013). Some studies suggest that there may be an acclimatization of species to CO_2 increase. Physiological processes often develop compensatory mechanisms that reduce or minimize the long-term effects of CO_2 (Dorneles *et al.* 2019). Acclimatization also may occur through the reduction of the maximum apparent rate of carboxylation (Ainsworth and Long 2021). An experiment with grasses suggested that the response to atmospheric CO_2 enrichment depends on the plant characteristics and environmental conditions, such as

patterns of water use and acquisition of nutrients, which may be the key to understanding changes in plant communities (Morgan *et al.* 2004). Although there are several experiments worldwide to evaluate the effect of higher atmospheric CO_2 on forests (Norby *et al.* 2005; Karnosky and Pregitzer 2006), there are still no long-term results for tropical forests regarding the behavior of carbon absorption.

As already mentioned, the photosynthesis in the ED2.2 model is controlled by the equations of Farquar (1980) and Leuning (1995). Leuning's equation indicates that, when moisture deficit increases, gs decreases. However, if there is an increase in environmental CO_2, gs decreases more sharply in this equation than in other equations, such as that of Ball and Berry (1987). Other ecosystem models that use the Ball and Berry equation do not consider the CO_2 compensation term, simulating lower gs values relative to the Leuning equation when there is high atmospheric CO_2 and low soil moisture. There are still no field data showing the combined effect of drought and increased CO_2 on tropical forests, therefore it is not yet possible to confirm whether the modelled results for the RCP4.5 and RCP8.5 scenarios are plausible. One of the main effects of the increase in CO_2 on plant carbon metabolism is the decrease in stomatal conductance (Leakey *et al.* 2009), although there is still no consensus on this subject.

A higher proportion of CO_2 in the atmosphere potentially increases photosynthetic activity, decreasing photorespiration and the Rubisco oxygenase activity (Buckeridge 2007). Another effect of increased atmospheric CO_2 is the increase in water use ratio between assimilated CO_2 and water loss. In our simulations, for RCP4.5 and 8.5, the water use efficiency increased by 24% in RCP4.5 and 31% in RCP8.5 relative to the control scenario. Possibly, biochemical damage occurred during leaf temperature increase due to the increase in ambient temperature, breaking or denaturing the enzymes involved in CO_2 fixation, causing photoinhibition or photodestruction (Roden *et al.* 1996). This result shows that, in a scenario with a high concentration of CO_2, there may be a limitation in the increase of carbon in the forest biomass, since the higher value of atmospheric CO_2 in the scenario RCP8.5 resulted in a lower GPP in relation to RCP4.5. The high levels of CO_2 in the atmosphere can, according to the GPP equation, contribute to the increase in forest biomass. In the GPP calculation, the CO_2 assimilation rate can implicitly ignore the limitation of low soil moisture conditions, causing vegetation to continue absorbing carbon beyond what would be expected for a drought condition. Plant respiration can increase exponentially with increasing temperature, however, photosynthetic rates are known to increase until they reach the ideal temperature and then decrease (Fitter 1981). For example, the photosynthetic activity of *Pistacia lentiscus* in the field was high when the temperature was below 30° C, and decreased above this limit, showing that the increase in

temperature influences the assimilation of CO_2 (Gatti *et al.* 2010).

An important consequence of the effect of increased atmospheric CO_2 on plant physiology is a decrease of rainfall in the Amazon. Simulations with the Brazilian Atmospheric Model (BAM) from CPTEC/INPE estimated that the impact of plant physiology on the amount of rain in the forest is greater than the effect of deforestation, through the reduction in canopy transpiration as a function of decreasing stomatal conductance driven by the increase in atmospheric CO_2 (Sampaio *et al.* 2021).

CONCLUSIONS

The majority of processes in the ED2.2 model, including photosynthesis, depend on soil moisture. Our results showed that the precipitation reduction in RCP4.5 and RCP8.5 scenario conditions can directly impact soil moisture, and thus can cause a cascade effect leading to the increase of matrix potential and reduction of stomatal conductance, thus transpiration and GPP, indicating that a drier and warmer climate may limit the plant growth. The variability in the availability of water can affect the rate of tree growth, as the precipitation is the principal source of soil moisture and consequently water for the vegetation. However, there is an important point to be considered in a scenario with warmer temperature and deficient rainfall. Does the increase in CO_2 concentration contribute to increase primary net production, as shown in our results? This is an important result from the projections, because an atmosphere enriched with CO_2 can promote changes in the metabolism and other physiological processes of the trees. This area needs further investigations. It is still not clear how the physiology of the tropical vegetation reacts when CO_2 concentration attains higher values along with changes in the rainfall and temperature patterns. The use of the field data combined with the simulations with robust models like ED2.2 can help answer how the stomatal conductance, the principal process involved in the accumulation of biomass, can be affected.

ACKNOWLEDGMENTS

REFERENCES

Ainsworth, E.A.; Long, S.P. 2021. 30 years of free-air carbon dioxide enrichment (FACE): what have we learned about future crop productivity and its potential for adaptation? *Global Change Biology*, 27: 27-49.

Anderegg, W.R.L.; Berry, J.A.; Smith, D.D.; Sperry, J.S.; Anderegg, L.D.L.; Field, C.B. 2012. The roles of hydraulic and carbon stress in a widespread climate induced forest die-off. *Proceedings of the National Academy of Sciences of the United States of America*, 109: 233–237.

Ball, J.T.; Woodrow, I.E.; Berry, J.A. 1987. A model predicting stomatal conductance and its contribution to the control of photosynthesis under different environmental conditions. In: Biggins, J. (Ed.). *Progress in Photosynthesis Research*, Springer, Dordrecht, p.221-224.

Betts, R.A.; Cox, P.M.; Collins, M.; Harris, P.P.; Huntingford, C.; Jones, C.D. 2004. The role of ecosystem-atmosphere interactions in simulated Amazon forest dieback under global climate warming. *Theoretical and Applied Climatology*, 78: 157-175.

Bonan, G.B. 1996. Sensitivity of a GCM simulation to subgrid infiltration and surface runoff. *Climate Dynamics*, 12: 279-285.

Braga, M.F. 2021. Revisão: Crescimento de plantas C3 e C4 em resposta a diferentes concentrações de CO_2. *Research, Society and Development*, 10: e33810716701.

Bruno, R.D.; da Rocha, H.R.; de Freitas, H.C.; Goulden, M.L.; Miller, S.D. 2006. Soil moisture dynamics in an eastern Amazonian tropical forest. *Hydrological Processes*, 20: 2477–2489.

Bustamante, J.F.; Gomes, J.L.; Chou, S.C.; Rozante, J.R. 1999. Evaluation of April 1999 rainfall forecasts over South America using. Climanálise,1999. 1-2 (http://climanalise.cptec.inpe.br/~rclimanl/revista/pdf/Eta_forecast_april99.pdf). Accessed on 21 May 2020.

Buckeridge, M.S.; Mortari, L.C.; Machado, M.R. 2007. Respostas fisiológicas de plantas às mudanças climáticas: alterações no balanço de carbono nas plantas podem afetar o ecossistema? Fenologia: ferramenta para conservação, melhoramento e manejo de recursos vegetais arbóreos. Embrapa Florestas. (https://repositorio.usp.br/item/002310032-livrofenologia). Accessed on 21 Jun 2020.

Chou, S.C.; Bustamante, J.F.; Gomes, J.L. 2005. Evaluation of Eta Model seasonal precipitation forecasts over South America. *Nonlinear Processes in Geophysics*, 12: 537-555.

Chou, S.C.; Lyra, A.; Mourão, C.; Dereczynski, C.; Pilotto, I.; Gomes, J.; *et al.* 2014. Assessment of climate change over South America under RCP 4.5 and 8.5 downscaling scenarios. *American Journal of Climate Change*, 3: 512-525.

Clapp, P.G.; Hornberger, G.M. 1978. Empirical equations for some soil hydraulic properties. *Water Resource Research*, 14: 601-604.

Cosby, B.J.; Hornberger, G.M.; Clapp, R.B.; Ginn, T. 1984. A statistical exploration of the relationships of soil moisture characteristics to the physical properties of soils. *Water Resources Research*, 20: 682-690.

Da Rocha, H.R.; Goulden, M.L.; Miller, S.D.; Menton, M.C.; Pinto, L.D.; de Freitas, H.C.; Silva Figueira, A.M. 2004. Seasonality of water and heat fluxes over a tropical forest in eastern Amazonia. *Ecological Applications*, 14(sp4): 22-32.

De Souza, E.B.; da Silva Ferreira, D.B.; Guimarães, J.T.F.; dos Santos Franco, V.; de Azevedo, F.T.M. 2017. Padrões climatológicos e tendências da precipitação nos regimes chuvoso e seco da Amazônia oriental. *Revista Brasileira de Climatologia*, 21: 81. doi:10.5380/abclima.v21i0.41232

Dorneles, K.R.; Posso, D.A.; Rebhahn, I.; Deuner, S.; Pazdiora, P.C.; Avila, L.A.; Dallagnol, L.J. 2019. Respostas morfofisiológicas

e rendimento de grãos do trigo mediados pelo aumento da concentração de CO_2 atmosférico. *Revista Brasileira de Ciências Agrárias*, 14: 1981-0997.

Doughty, C.E.; Metcalfe, D.B.; Girardin, C.A.; Amezquita, F.F.; Cabrera, D.G.; Huasco, W.H.; *et al*. 2015. Drought impact on forest carbon dynamics and fluxes in Amazonia. *Nature*, 519: 78–82.

Espírito-Santo, F.D.B.; Shimabukuro, Y.E.; Aragão, L.E.O.; & Machado, E.L.M. 2005. Análise da composição florística e fitossociológica da floresta nacional do Tapajós com o apoio geográfico de imagens de satélites. *Acta Amazonica*, 35: 155-173.

Farquhar, G.; von Caemmerer, S.; Berry, J. 1980. A biochemical model of photosynthetic CO_2 assimilation in leaves of C3 species, *Planta*, 149: 78–90.

Felsemburgh, C.A. 2009. Respostas fotossintéticas à variação da temperatura foliar do dossel na Flona do Tapajós - PA. Doctoral thesis, Universidade de São Paulo, Brazil, 117p. (https://www.teses.usp.br/teses/disponiveis/91/91131/tde-14092009-082158/pt-br.php)

Field, C.B.; Jackson, R.B.; Mooney, H.A. 1995. Stomatal responses to increased CO_2: implications from the plant to the global scale. *Plant, Cell and Environment*, 18: 1214-1225.

Ficklin, D.L; Novick, K.A. 2017. Historic and projected changes in vapor pressure deficit suggest a continental-scale drying of the United States atmosphere. *Journal of Geophysical Research: Atmospheres*, 122: 2061–2079.

Fitter, A.H.; Hay, R.K.M. 1987. Environmental Physiology of Plants. Academic Press, London, 367p.

Franklin, J.F.; MacMahon, J.A.; Swanson, F.J.; Sedell, J.R. 1985. Ecosystem responses to the eruption of Mount St. Helens. *National Geographic Research*, 1: 198-216.

Furtado, A.T.; Júnior, M.J.A.F.; Dill, T.; Valente, F.; Cosme, R.; Moura, J.M.; *et al*. 2013. Influência da umidade no efluxo de CO_2 do solo para atmosfera em uma área de floresta primária, Belterra, PA. *Ciência e Natura*, 2013-12: 25-27.

Gatti, E.; Rossi, F. 2010. Daily and seasonal trends of gas exchange in *Pistacia lentiscus* L. *Acta Physiologiae Plantarum*, 32: 809-813.

Hawkins, E.; Ortega, P.; Suckling, E.; Schurer, A.; Hegerl, G., Jones, P.; Van Oldenborgh, G.J. 2017. Estimating changes in global temperature since the preindustrial period. *Bulletin of the American Meteorological Society*, 98: 1841-1856.

Islam, H.; Soares, C.G.; Liu, J.; Wang, X. 2021. Propulsion power prediction for an inland container vessel in open and restricted channel from model and full-scale simulations. *Ocean Engineering*, 229: 108621.

Karnosky, D.F.; Pregitzer, K.S. 2006. Impacts of elevated CO_2 and O_3 on northern temperate forest ecosystems: results from the Aspen FACE experiment. In: Nösberger, J.; Long, S.P.; Norby, R.J.; Stitt, M.; Hendrey, G.R.; Blum, H. (Ed.). *Managed Ecosystems and CO_2*, Springer, Berlin, p.213-229.

Kooperman, G.J.; Chen, Y.; Hoffman, F.M. 2018. Forest response to rising CO_2 drives zonally asymmetric rainfall change over tropical land. *Nature Climate Change*, 8: 434–440.

Leakey, A.D.; Ainsworth, E.A.; Bernacchi, C.J.; Rogers, A.; Long, S.P.; Ort, D.R. 2009. Elevated CO_2 effects on plant carbon, nitrogen, and water relations: six important lessons from FACE. *Journal of Experimental Botany*, 60: 2859-2876.

Leuning, R. 1995. A critical appraisal of a combined stomatal-photosynthesis model for C3 plants. *Plant, Cell and Environment*, 18: 339–355.

Liberato, A.M.; Brito, J.I.B. 2010. Influência de mudanças climáticas no balanço hídrico da Amazônia Ocidental. *Revista Brasileira de Geografia Física*, 3: 170-180.

Lloyd, J.; Farquhar, G.D. 2008. Effects of rising temperatures and $[CO_2]$ on the physiology of tropical forest trees. *Philosophical Transactions of the Royal Society B: Biological Sciences*, 363: 1811-1817.

Longo, M.; Keller, M.; dos-Santos, M.N.; Leitold, V.; Pinagé, E.R.; Baccini, A.; Morton, D.C. 2016. Aboveground biomass variability across intact and degraded forests in the Brazilian Amazon. *Global Biogeochemical Cycles*, 30: 1639-1660.

Longo, M.; Knox, R.G.; Medvigy, D.M.; Levine, N.M.; Dietze, M.C.; Kim, Y.; Moorcroft, P.R. 2019. The biophysics, ecology, and biogeochemistry of functionally diverse, vertically and horizontally heterogeneous ecosystems: The Ecosystem Demography model, version 2.2–Part 1: Model description. *Geoscientific Model Development*, 12: 4309-4346.

Lyra, A. de A.; Chou, S.C.; Sampaio, G. de O. 2016 Sensitivity of the Amazon biome to high resolution climate change projections, *Acta Amazonica*, 46: 175–188.

McDowell, N.G. 2011. Mechanisms linking drought, hydraulics, carbon metabolism, and vegetation mortality. *Plant Physiology*, 155: 1051–1059.

Medvigy, D.; Wofsy, S. C.; Munger, J. W.; Hollinger, D. Y.; & Moorcroft, P. R. 2009. Mechanistic scaling of ecosystem function and dynamics in space and time: Ecosystem Demography model version 2. *Journal of Geophysical Research: Biogeosciences*, 114(G1).

Moorcroft, P.R.; Hurtt, G.C.; Pacala, S.W. 2001. A method for scaling vegetation dynamics: The Ecosystem Demography model (ED). *Ecological Monographs*, 71: 557-587.

Morgan, J.A.; Pataki, D.E; Körner, C.; Clark, H.; Del Grosso, S.J.; Grünzweig, J.M.; *et al*. 2004. Water relations in grassland and desert ecosystems exposed to elevated atmospheric CO_2. *Oecologia*, 140: 11-25.

Nepstad, D.C.; Moutinho, P.; Dias-Filho, M.B.; Davidson, E.; Cardinot, G.; Markewitz, D.; *et al*. 2002. The effects of partial throughfall exclusion on canopy processes, aboveground production, and biogeochemistry of an Amazon forest. *Journal of Geophysical Research*: *Atmospheres*, 107: LBA-53-1-18.

Nepstad, D.; Moutinho, P.; Brando, P. 2013. LBA-ECO CD-05 Soil VWC and Meteorology, Rainfall Exclusion, Tapajos National Forest. Data set. (https://doi.org/10.3334/ORNLDAAC/1169).

Norby, R.J.; DeLucia, E.H.; Gielen, B.; Calfapietra, C.; Giardina, C.P.; King, J.S.; Oren, R. 2005. Forest response to elevated CO_2 is conserved across a broad range of productivity. *Proceedings of the National Academy of Sciences*, 102: 18052-18056.

Nobre, C.A.; Sampaio, G.; Salazar, L. 2007. Mudanças climáticas e Amazônia. *Ciência e Cultura*, 59: 22-27.

Paiva, A.S.; Fernandes, E.J.; Rodrigues, T.J.; Turco, J.E. 2005. Stomatal conductance in leaves of bean plants submitted to different irrigation regimes. *Engenharia Agrícola*, 25: 161-169.

Piao, S.; Ciais, P.; Friedlingstein, P.; de Noblet-Ducoudré, N.; Cadule, P.; Viovy, N.; Wang, T. 2009. Spatiotemporal patterns of terrestrial carbon cycle during the 20th century. *Global Biogeochemical Cycles,* 23: GB4026.

Powell, T.L.; Galbraith, D.R.; Christoffersen, B.O.; Harper, A.; Imbuzeiro, H.M.; Rowland, L.; Moorcroft, P.R. 2013. Confronting model predictions of carbon fluxes with measurements of Amazon forests subjected to experimental drought. *New Phytologist*, 200: 350-365.

Restrepo-Coupe, N.; Da Rocha, H.R.; Hutyra, L.R.; Da Araujo, A.C.,; Borma, L.S.; Christoffersen, B.; Saleska, S.R. 2013. What drives the seasonality of photosynthesis across the Amazon basin? A cross-site analysis of eddy flux tower measurements from the Brasil flux network. *Agricultural and Forest Meteorology*, 182: 128-144.

Restrepo-Coupe, N.; Levine, N.M.; Christoffersen, B.O.; Albert, L.P.; Wu, J.; Costa, M.H.; Saleska, S.R. 2017. Do dynamic global vegetation models capture the seasonality of carbon fluxes in the Amazon basin? A data-model intercomparison. *Global Change Biology*, 23: 191-208.

Roden, J.S.; Ball, M.C. 1996. The effect of elevated [CO_2] on growth and photosynthesis of two eucalyptus species exposed to high temperatures and water deficits. *Plant Physiology*, 111: 909-919.

Rowland, L.; da Costa, A.C.; Galbraith, D.R.; Oliveira, R.S.; Binks, O.J.; Oliveira, A. A.; Meir, P. 2015. Death from drought in tropical forests is triggered by hydraulics not carbon starvation. *Nature*, 528: 119-122.

Saleska, S.; da Rocha, H.; Kruijt, B.; Nobre, A. 2009. Ecosystem carbon fluxes and Amazonian forest metabolism. *Geophysical Monograph Series*, 186, 389-407.

Sampaio, G.; Shimizu, M.H.; Guimarães-Júnior, C.A.,; Alexandre, F.; Guatura, M.; Cardoso, M.; Lapola, D.M. 2021. CO_2 physiological effect can cause rainfall decrease as strong as large-scale deforestation in the Amazon. *Biogeosciences,* 18: 2511-2525.

Sellers, P.J.; Randall, D.A.; Collatz, G.J.; Berry, J.A.; Field, C.B.; Dazlich, D.A.; Bounoua, L. 1996. A revised land surface parameterization (SiB2) for atmospheric GCMs. Part I: Model formulation. *Journal of climate*, 9: 676-705.

Silva, F.B. 2013. Modelagem da produtividade primária na Bacia Amazônica. Doctoral thesis, Instituto Nacional de Pesquisas Espaciais, Brazil, 120p. (http://urlib.net/sid.inpe.br/mtc-m19/2013/06.20.13.35). Accessed on 24 Jan 2021.

Yang, Z.D.; Robert, H.S.; An, A. 1995. Preliminary study of spin-up processes in land surface models with the first stage data of Project for Intercomparison of Land Surface Parameterization Schemes Phase 1(a). *Journal of Geophysical Research.* 1001: 16553-16578.

Zandalinas, S.I.; Fritschi, F.B.; Mittler, R. 2021. Global warming, climate change, and environmental pollution: recipe for a multifactorial stress combination disaster. *Trends in Plant Science*, 26: 588-599.